RM No. L9B24a

NACA

RESEARCH MEMORANDUM

AN EXPERIMENTAL INVESTIGATION OF A GYRO-ACTUATED ROLL CONTROL SYSTEM INSTALLED IN A SUBSONIC TEST VEHICLE

By

Jerome M. Teitelbaum and Ernest C. Seaberg

Langley Aeronautical Laboratory
Langley Air Force Base, Va.

NATIONAL ADVISORY COMMITTEE
FOR AERONAUTICS

WASHINGTON

April 20, 1949
Declassified July 29, 1954

NATIONAL ADVISORY COMMITTEE FOR AERONAUTICS

RESEARCH MEMORANDUM

AN EXPERIMENTAL INVESTIGATION OF A GYRO-ACTUATED ROLL CONTROL SYSTEM INSTALLED IN A SUBSONIC TEST VEHICLE

By Jerome M. Teitelbaum and Ernest C. Seaberg

SUMMARY

The results of subsonic wind-tunnel and flight tests of a gyro-actuated roll control system installed in a tailless subsonic test vehicle having an elliptical body-of-revolution-type fuselage and sweptback wings are presented herein. The wind-tunnel tests were conducted in the high-speed 7- by 10-foot tunnel at the NACA Langley Laboratory, and the model was launched in free flight at the NACA Pilotless Aircraft Research Station at Wallops Island, Va.

The gyro-actuated control system employed in these tests to obtain roll stabilization of the model is a system which links the control surface directly to the displacement gyroscope and employs a torque motor to limit gyroscope precession. The linking of the control surfaces directly to the gyroscope results in an autopilot system which gives a no-lag control response to a model displacement without resorting to velocity or acceleration-sensitive devices.

The results of the tests conducted indicate that the gyro-actuated control system is a practical method for obtaining roll stabilization of pilotless aircraft. In application of this system, the control-surface hinge moment of the test vehicle determines the output requirements of the torque motor while the precession rate of the gyroscope caused by this hinge moment determines the required response characteristics of the torque motor.

INTRODUCTION

As part of the general research program on guided missiles, the NACA has been conducting a series of automatic stabilization tests employing various autopilot systems installed in a subsonic rocket-propelled test vehicle. In the initial unpublished phase of the program, flight tests were conducted using a modified German V-1 autopilot consisting of a two-gimbal air-driven displacement gyroscope

and air-driven rate gyroscopes actuating pneumatic servomotors for yaw and pitch control. Roll stabilization was obtained by use of electrically operated displacement and rate gyroscopes actuating flicker-pneumatic servomotors. In another test, systems for pitch, yaw, and roll control based on the roll-stabilization method used in the initial tests were employed. In these tests, stabilization of the model in all three controlled planes was not obtained because of operational failures of one or more of the many components required to construct each system.

In an attempt to construct an autopilot system capable of satisfying the rapid autopilot response requirements needed for supersonic flight of pilotless aircraft, and at the same time simplifying the control mechanism, the tests reported herein were conducted employing a gyro-actuated control system in order to obtain roll stabilization. This system, which links the control surface directly to a displacement gyroscope and has a torque motor to limit gyroscope precession, eliminates the need for a rate gyroscope and replaces a precision servomotor with a slower-acting torque motor. By linking the control surface directly to the gyroscope, it is possible to approximate a no-lead no-lag autopilot system without resorting to velocity or acceleration-sensitive devices.

In these tests, no attempt was made to control the model in pitch and yaw. Initially, a theoretical investigation was conducted based on the assumption that the model-autopilot combination was a single degree-of-freedom system in roll. Tests of the model having freedom in roll were then conducted in the Langley high-speed 7- by 10-foot tunnel, and the results of the tests compared to the theoretical analysis. Finally, the model was tested in free flight.

APPARATUS

Autopilot

The autopilot used in the present tests was designed to stabilize the model in roll only. The system employed is one which directly couples the gyroscope to the control surface, as shown in figures 1 and 2. A commercial aircraft directional stability autopilot was modified by the Instrument Research Division of the Langley Laboratory for these initial tests of the system. The autopilot, contained a two-gimbal gyroscope, which was so positioned that the outer gimbal was alined with the longitudinal axis of the model in order to maintain freedom in roll, and the inner gimbal was alined to have freedom in the yawing plane. A cam was rigidly attached to the outer gimbal so that the cam would maintain its roll position in space regardless of the

roll attitude of the model. Through a series of linkages, the roll control surfaces were meshed with the cam. Change in roll attitude of the model moved the linkage attachment position on the cam in such a manner as to give a specific amount of control-surface deflection per degree of roll displacement. Three different cams were constructed having values of control gearing ratio K (the ratio of the total aileron deflection per degree roll displacement) equal to 2, 1, and $\frac{1}{2}$. In all three cases, the cams were designed to limit the total aileron control deflection to 20° for roll in either direction. Should the model roll 180°, the cams were designed to cause the control-surface deflection to reverse and continue the roll until the model returned to the zero roll position.

In operation, the control-surface deflection would cause a hinge moment to be transmitted to the gyroscope through the linkage and cam. This hinge moment or torque, when applied to the outer gimbal of the gyroscope, caused a precession of the inner gimbal in the yaw plane. Electrical pickoffs, which were located to detect the yaw displacement of the gyroscope, actuated the friction clutch of a torque motor in such a manner as to apply a counteracting torque in order to stop the precession of the gyroscope and, therefore, basically supply the energy required to overcome the hinge moments of the deflected control surfaces. These electrical pickoffs were so constructed that the moment created on the inner gimbal by them would be negligible, and with a sufficient dead spot region to eliminate the possibility of the torque motor hunting. During operation, any play in the control linkage would cause a decrease in the effective control gearing ratio without affecting the phasing of the control response to model displacement as the control hinge moments tend to keep the linkage tight.

The action of this roll system is unaffected by yaw and pitch of the model when they occur independently. However, under the combined action of the model in pitch and yaw the gyroscope will lose its roll reference as this is an inherent limitation of a free gyroscope. The action of the torque motor is advantageous, however, since it maintains a perpendicular relation between the inner and outer gimbals, thus preventing locking of the gimbals.

For these tests, a gyroscope having an angular momentum of 4.71 foot-pound-seconds was employed and the torque motor was capable of producing approximately 45 inch-pounds of torque to the outer gimbal of the gyroscope through a friction clutch.

Model

The model used for these tests was essentially a tailless airplane with sweptback cruciform wings. The model was launched from a zero-length launching rack with the aid of a four-fin booster containing a

rocket motor delivering 10,000 pounds of thrust for 1.8 seconds. After booster burn-out and separation, the model maintained a flight velocity of approximately 600 feet per second with the aid of an internal sustainer rocket motor producing about 200 pounds of thrust for 45 seconds.

A sketch of the model and booster is shown in figure 3 and the physical characteristics are given in table I.

Wind-Tunnel Tests

The model was installed in the wind-tunnel on fore-and-aft supports as shown in figure 4 to permit roll freedom and was instrumented to record the following:

(1) Right horizontal aileron position

(2) Lower vertical aileron position

(3) Angle of bank

(4) Torque motor signal for counterclockwise gyroscope precession

(5) Torque motor signal for clockwise gyroscope precession

Wind-tunnel tests were conducted with the autopilot containing each cam (that is, having control gearing ratios of 2, 1, or $\frac{1}{2}$ at various Mach numbers from 0.5 to 0.7).

Flight Test

For the flight test, the autopilot with the cam having a control gearing ratio of 2 was employed. A pulsing unit was installed to disturb the model in roll. This unit, powered by a pneumatic servo, caused the vertical ailerons to move intermittently between 0° and 12° total aileron deflection for intervals of 4 and 2 seconds, respectively.

A six-channel telemeter was installed in the model to transmit to recording stations located near the launching site the following items within the limits noted between the parenthesis signs:

(1) Lower vertical control position (-12° to +6°)

(2) Right horizontal control position (±10°)

(3) Angle of bank (±24°)

(4) Dynamic pressure (0 to 15 inches Hg above static pressure)

(5) Transverse acceleration (-5g to +15g)

(6) Rate of roll (±100°/sec)

In flight, the model was tracked by radar to determine the flight path. In addition, one 16-millimeter high-speed and two 16-millimeter color cameras were used to obtain motion-picture records of the flight.

RESULTS AND DISCUSSION

In order to calculate the response of the model with the gyro-actuated control system, it was necessary to make the assumption that the control motion was in phase with the rolling motion. The use of this assumption simplified the roll equation of motion so that an analytic solution could be applied without having to resort to a graphical analysis. The method used to calculate the response of the model to a disturbance is shown in the appendix. For this anlysis, the values of the damping moment due to the rolling velocity L_{ϕ} and the rolling moment due to aileron control deflection L_{δ_a} were obtained from the 7- by 10-foot wind-tunnel tests of the model. The moment of inertia was experimentally determined. A plot of the calculated response of the model to a roll displacement of 10° is shown in figure 5 as functions of the control gearing ratio K for a theoretical flight Mach number of 0.6. From the plot of the curves in figure 5 it can be seen that increasing the control gearing ratio tends to increase the operating frequency without affecting the damping of the system.

Wind-Tunnel Tests

The wind-tunnel tests were conducted for the model-autopilot combination through a Mach number range of 0.5 to 0.7. The tests were made through the speed range for each cam installation so that the effect of varying the control gearing ratio could be verified. During the test runs, the model was displaced in roll by manually applying a rolling moment through cables attached to the wing tips. Records of the return of the model to its zero roll reference from the displaced position were taken and are shown in figure 6. During the tests, the model did not trim at the zero roll reference but at an angle of bank at which the moment due to the control deflection counteracted the moment due to model misalinement. For the test runs shown in figures 6(a), (b), and (c), trim corrections could be estimated from the data and the theoretical response curves plotted include these corrections.

Also affecting the response of the model was the roughness of flow in the test section of the tunnel due to the comparatively large model size. This gust condition disturbed the model in some of the tests to the extent that the results could not be compared with a theoretical analysis. In figures 6(d) and (e), the results indicate that a gust disturbed the model during the response and no accurate estimate of the trim correction could be made. The theoretical curves in these cases were calculated having no trim corrections.

Comparison of the theoretical with the experimental response curves shows the oscillating frequency of the model to be higher than predicted in the theoretical analysis which indicates that the value used for KL_{δ_a} may have been too low. As K is a constant dependent on the cam employed, the discrepancy of the oscillating frequency noted appears to be due to the value used for L_{δ_a}. This is further substantiated in figures 6(b), (d), and (e) because the frequency of the experimental curves in these figures varies approximately as the square root of K, which is valid when the frequency is determined from equation (8) in the appendix and the damping term $\left(\frac{L\dot{\phi}}{I_x}\right)^2$ is neglected.

Flight Tests

Test records and motion pictures of the flight showed that the launching was smooth, and the model attained an altitude of about 460 feet before booster burn-out and separation. The profile view of the take-off of the model was obtained from the radar data and is shown in figure 7. The horizontal control surfaces were designed for combined elevator and aileron controls and for this test a 2.5° up-elevator control setting in these control surfaces caused the model to fly in a flattened projectile trajectory for approximately 35 seconds.

The telemeter record indicated that the pulse mechanism failed in operation 9 seconds prior to firing, and the vertical aileron controls remained at zero deflection. Of the remaining channels, the rate-of-roll indicator operated improperly, and the entire telemeter failed after 7.8 seconds of flight. However, sufficient data were obtained to show how the autopilot operated during boosted flight and for a short period of time after sustainer ignition. The data obtained from the telemeter record, presented in figure 8, show that there was a slight roll oscillation during boosted flight and immediately after the sustainer was ignited. This oscillation damped out at approximately 4.2 seconds, and the model flew with the left wing down about 2° after this time. The maximum airspeed attained was 660 feet per second which was equivalent to a Mach number of 0.577.

For these tests, the over-all telemeter accuracy is based on the maximum range of the individual channels. For the angle-of-bank channel, telemeter accuracy was ±0.7°, while the accuracy of the total horizontal aileron deflection was ±1.2°. The error involved in reading up the record

therefore could be of the magnitude given above. However, the relative error of the point-to-point read-up of the individual channels was ±0.2° for the angle of bank and the total aileron deflection records. By comparing the angle of bank and the aileron-control-deflection records, it can be seen that they were operationally in phase. No evaluation on the control gearing ratio could be made as failure of the pulsing mechanism reduced the disturbance to values where the telemeter accuracy limited the ability to compare the roll disturbance to the amount of control deflection.

For the remainder of the flight, although no telemeter data were available, the motion pictures showed no discernible roll.

CONCLUDING REMARKS

The gyro-actuated control system appears to be a practical method for obtaining roll stabilization of a subsonic pilotless aircraft. Wind-tunnel and flight tests show that the system is one in which the control response is in phase with the model displacement. In order to apply the system to a supersonic vehicle, an analysis of the system would have to be made in which the equations of motion would be evaluated for the specific vehicle at the desired operating velocity. In any case, the degree of stability of the model-autopilot combination would be a function of the amount of aerodynamic damping and the control effectiveness of the model. Additional trials of this system, particularly in supersonic vehicles, appear warranted.

In application of this system, the control-surface hinge moment of the test vehicle determines the output requirements of the torque motor, while the precession rate of the gyroscope caused by this hinge moment determines the required response characteristics of the torque motor.

Langley Aeronautical Laboratory
National Advisory Committee for Aeronautics
Langley Air Force Base, Va.

APPENDIX

METHOD FOR CALCULATING THEORETICAL ROLL RESPONSE OF MODEL WITH A GYRO-ACTUATED CONTROL SYSTEM

The autopilot was designed with interchangeable cams to obtain selective proportionality between the angle of bank and control deflection. Each cam maintained its control gearing ratio between the limits of $\pm 20^\circ$ total aileron deflection. At these limits, the aileron deflection remained constant with increase in angle of bank. In order to represent this in the analysis, the equations were set up for the following conditions:

Condition 1 - Constant aileron control; $\delta_a = 20^\circ$

Condition 2 - Proportion aileron control; $\delta_a = -K\phi$

In addition, the assumption that there was no phase shift between the angle of bank and the control deflection was made.

In order to correct the results for construction misalinement which caused an out-of-trim rolling moment L_T to be imposed on the model during the tests, it was necessary that the trim angle ϕ_T be obtained from the test records. From this information the out-of-trim moment was calculated to be

$$L_T = \phi_T K L_{\delta_a} \tag{1}$$

The equation for the roll response of the model for one degree of freedom is

$$I_x D^2\phi - L_{\dot{\phi}} D\phi - \delta_a L_{\delta_a} - L_T = 0 \tag{2}$$

Solution of this equation for condition 1 yields

$$\phi = \frac{\left(\delta_a L_{\delta_a} + L_T\right) I_x}{L_{\dot{\phi}}^2} \left[e^{\frac{L_{\dot{\phi}}}{I_x} t} - \frac{L_{\dot{\phi}}}{I_x} t - 1 \right] + \phi_o \tag{3}$$

$$D\phi = \frac{\delta_a L_{\delta_a} + L_T}{L_{\dot{\phi}}} \left[e^{\frac{L_{\dot{\phi}}}{I_x} t} - 1 \right] \tag{4}$$

For condition 2, equation (2) takes the form :

$$\left(I_x D^2 - L_{\dot{\phi}} D + KL_{\delta_a}\right)\phi = L_T \tag{5}$$

which has as its solution

$$\phi = e^{-At}\left[\left(\phi_e - \frac{L_T}{KL_{\delta_a}}\right)\cos Bt + \left(\phi_e - \frac{L_T}{KL_{\delta_a}} + \frac{D\phi_e}{A}\right)\frac{A}{B}\sin Bt\right] + \frac{L_T}{KL_{\delta_a}} \tag{6}$$

where

$$A = -\frac{L_{\dot{\phi}}}{2I_x} \tag{7}$$

$$B = \frac{1}{2}\sqrt{\frac{4KL_{\delta_a}}{I_x} - \left(\frac{L_{\dot{\phi}}}{I_x}\right)^2} \tag{8}$$

and ϕ_e and $D\phi_e$ are determined from the end conditions obtained from equations (3) and (4) of condition 1.

From equation (6) a plot of ϕ against time can be made for the condition where the aileron deflection is proportional to the angle of bank. Using this, combined with a plot of equation (3), the entire plot of the roll response of the model can be obtained, examples of which are shown in figure 6.

The quantities used in the foregoing calculations are as follows:

ϕ angle of bank, radians

ϕ_o initial angle of bank, radians

ϕ_e final angle of bank determined from condition 1, radians

ϕ_T trim angle of bank, radians

δ_a total aileron control deflection, radians

L_{δ_a} rate of change of rolling moment with total aileron control deflection, foot-pounds per radian $\left(\frac{\partial L}{\partial \delta_a}\right)$

$L_{\dot{\phi}}$ rate of change of rolling moment with angular rolling velocity, foot-pounds per radian per second $\left(\frac{\partial L}{\partial D\phi}\right)$

L_T out-of-trim moment, foot-pounds

I_x moment of inertia about longitudinal body axis, slug-feet^2

e natural logarithm (2.7183)

t time, seconds

K control gearing ratio $\left(K = -\frac{\delta_a}{\phi}\right)$

D differential operator $\left(\frac{d}{dt}\right)$

A,B constants

M Mach number

TABLE I

PHYSICAL DIMENSIONS OF TEST VEHICLE

Model weight, pounds:	
For wind-tunnel tests	192
For flight test, loaded	468
Booster weight, pounds	400
Wing:	
Area, square feet (including fuselage)	7.13
Span, feet	5.72
Aspect ratio	4.58
Airfoil section	NACA 16-009
Root chord, inches	21.88
Tip chord, inches	6.09
Taper ratio	0.278
Mean aerodynamic chord, inches	15.70
Sweepback, 25-percent chord, degrees	41
Incidence, degrees	0
Wing loading (model only), pounds per square foot	65.7
Control surface:	
Type	Plain flap
Span, percent wing span (plan)	23
Chord, percent wing chord at inboard end	15.7
Chord, percent wing chord at outboard end	26.7
Fuselage:	
Length, inches	120
Maximum diameter, inches	20
Center-of-gravity location:	
Behind nose of fuselage, inches	66
Above center line of model, inches:	
For wind-tunnel tests	0.41
For flight test	0.17
Rolling moment of inertia I_x, slug-feet^2:	
For wind-tunnel tests	6.95
For flight test	7.30

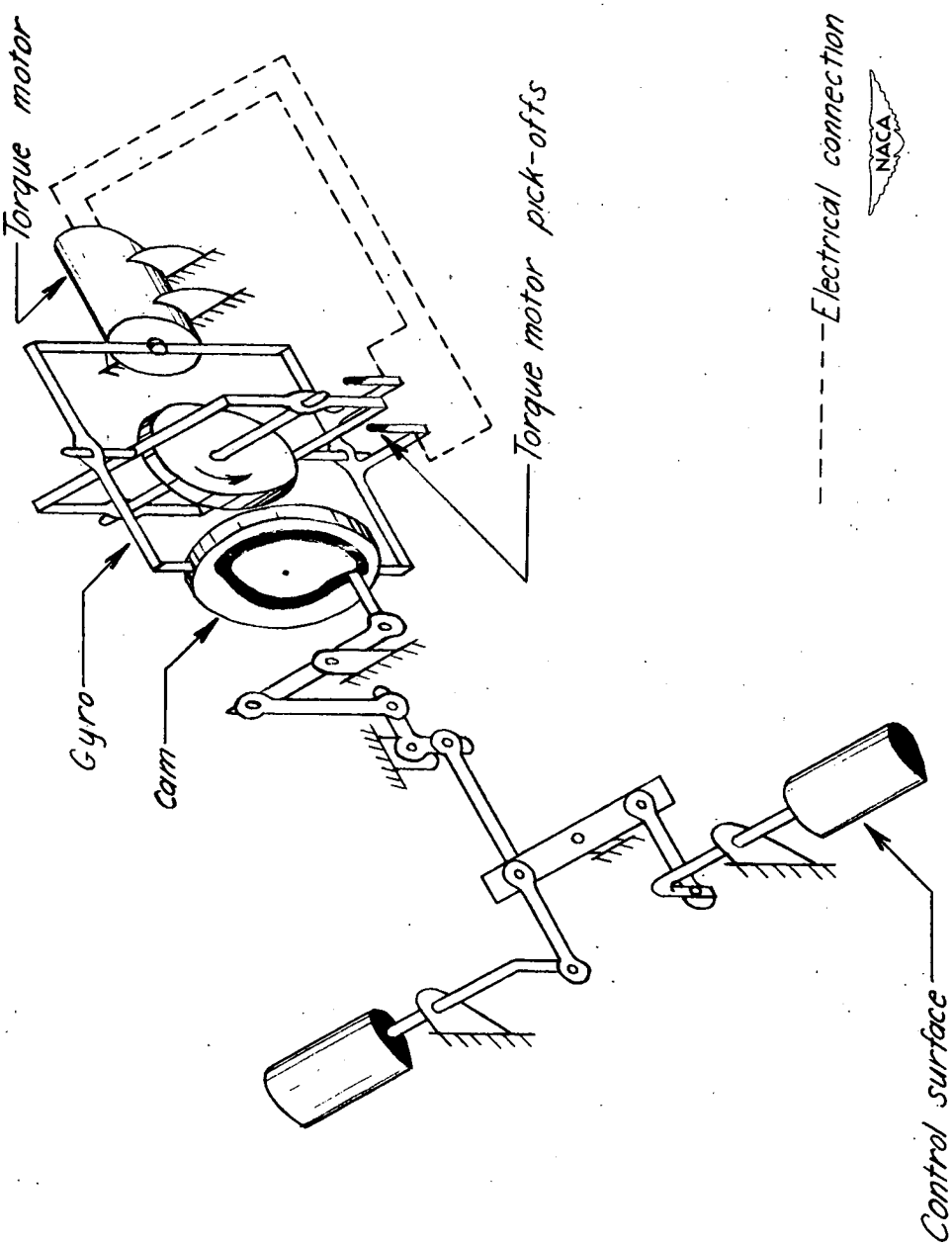

Figure 1.- Schematic diagram of the gyro-actuated control system used for roll stabilization.

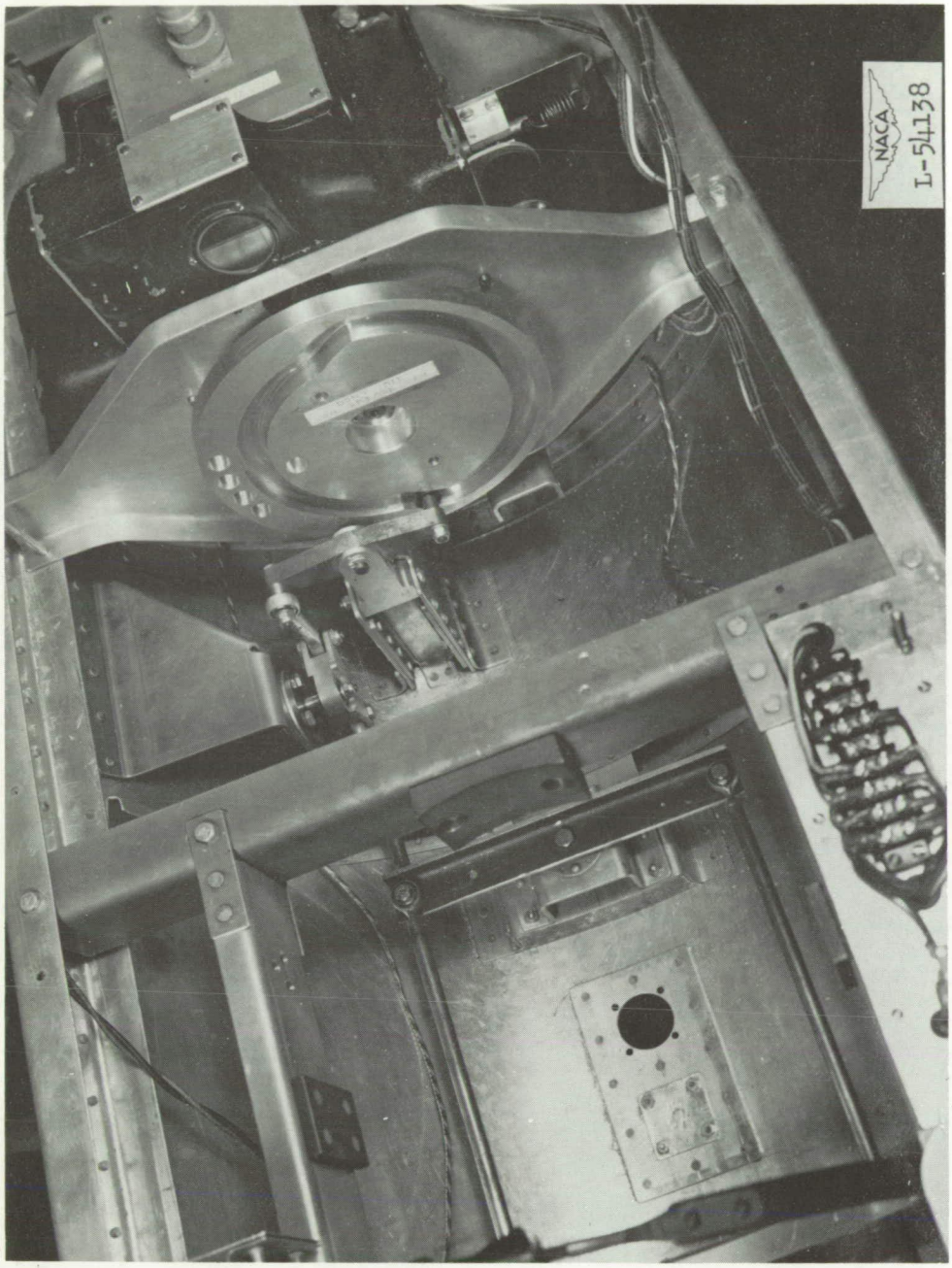

Figure 2.- Internal view of the model showing linkage, cam, and gyro.

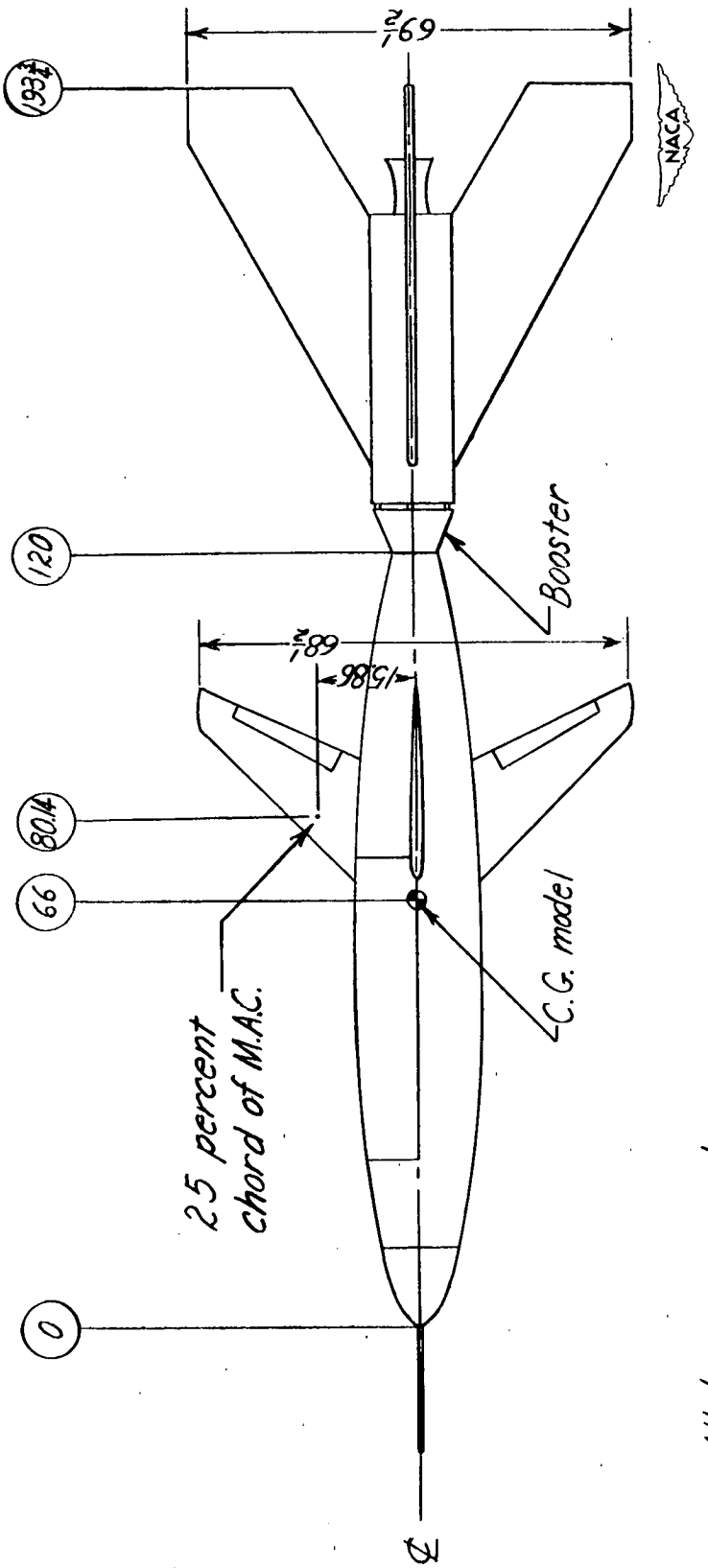

All dimensions in inches

Figure 3. - Sketch of subsonic test vehicle and booster.

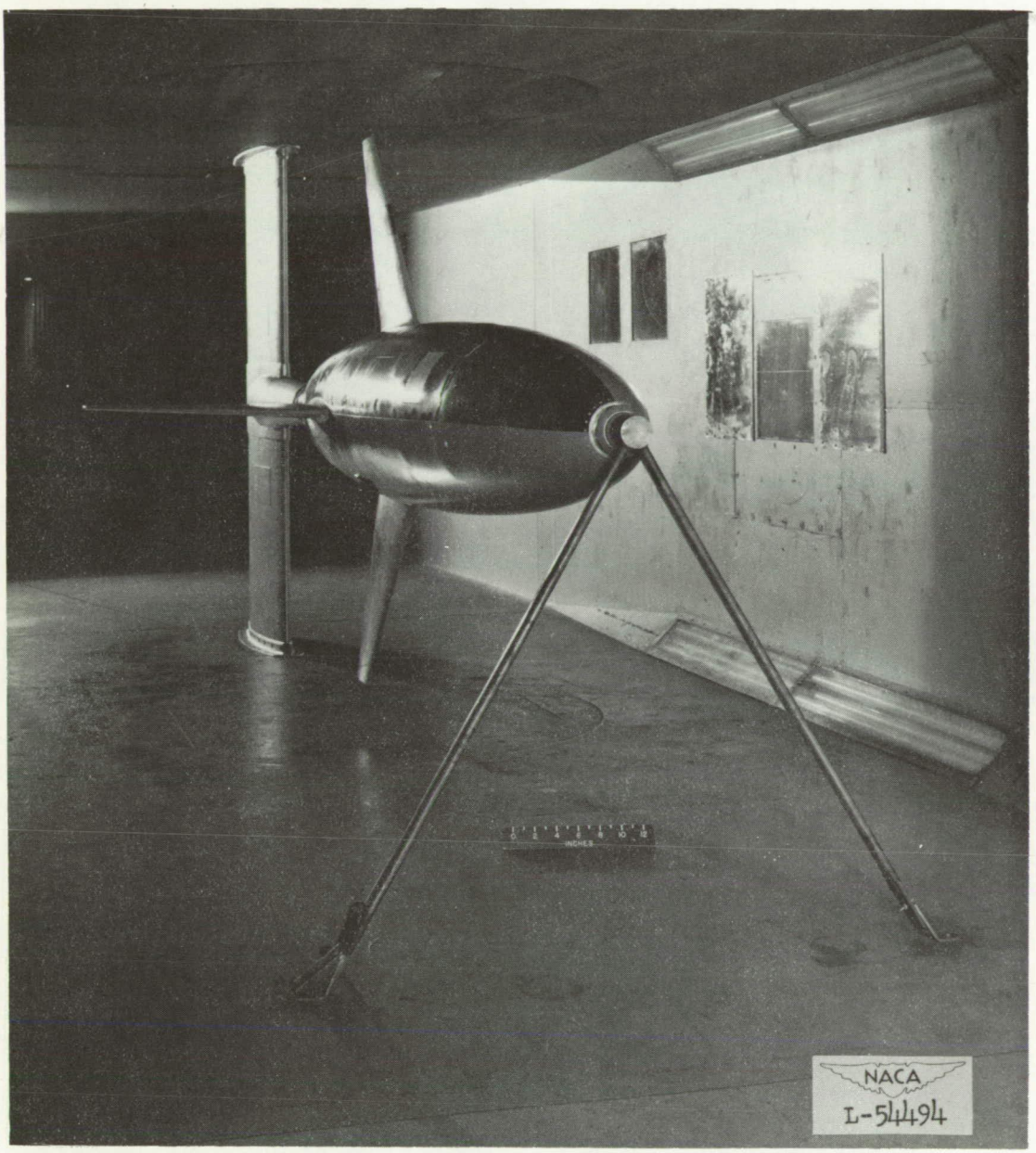

Figure 4.- Wind-tunnel installation of the model.

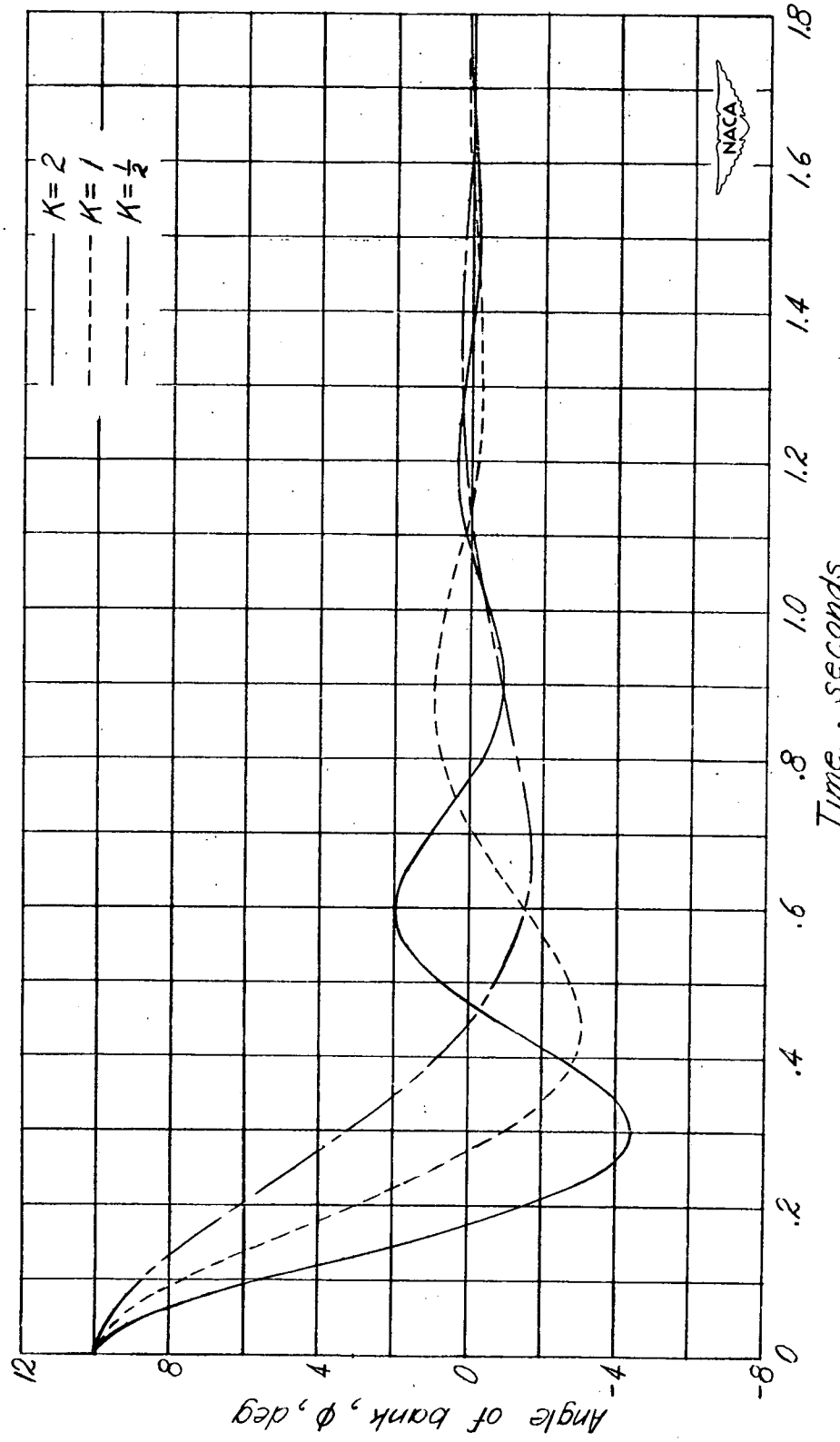

Figure 5. - Calculated effect of varying the autopilot control gearing ratio (K) on the theoretical response of the model to an initial roll displacement of 10° at a Mach number of 0.6, $L_{\dot{\phi}}$ of -37.67 ft-lbs/rad/sec and L_{δ_a} of 407 ft-lbs/rad.

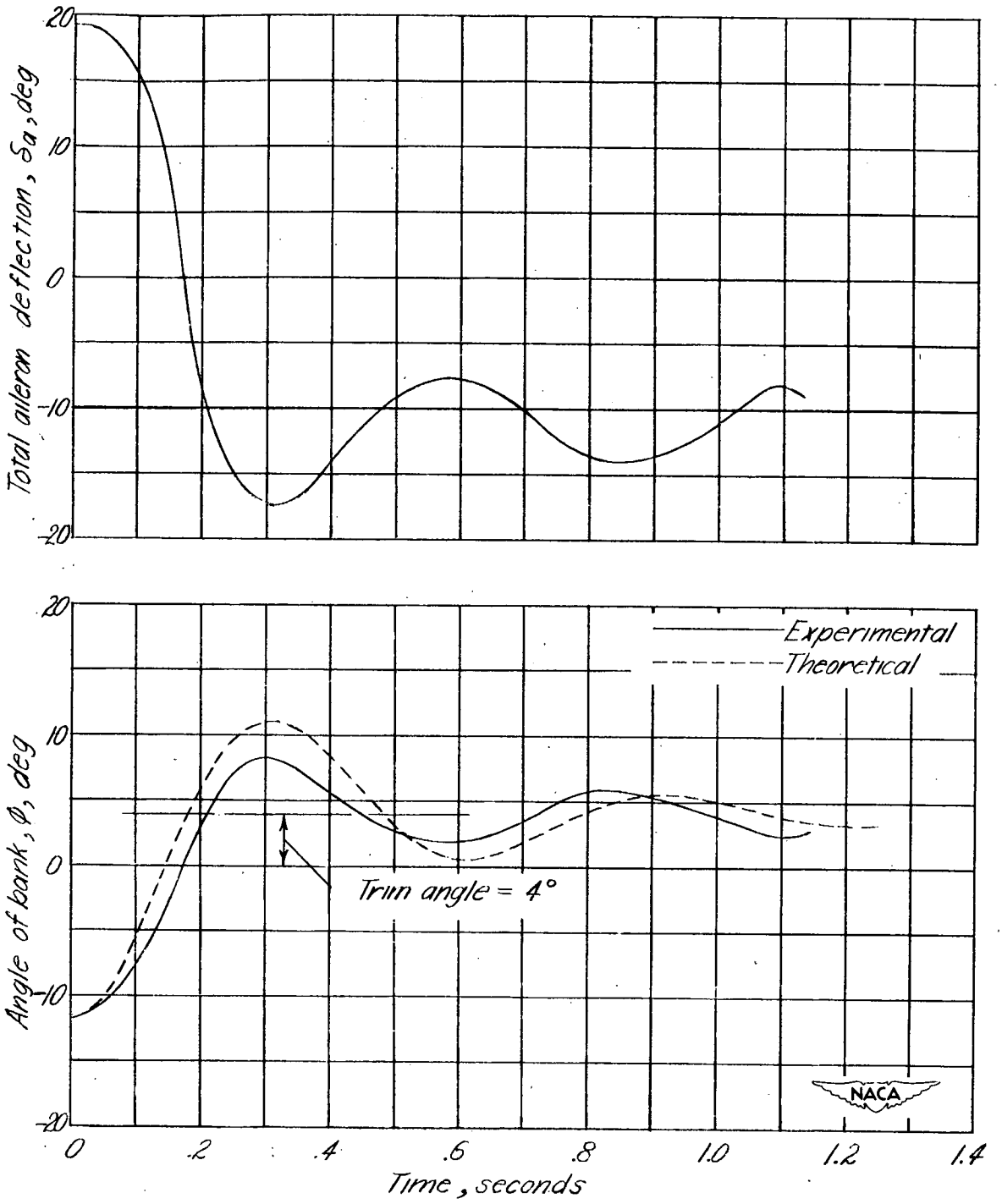

(a) $K=2$; $M=0.55$; $L_{\dot{\phi}} = -35$ ft-lbs/rad/sec ; $L_{\delta_a} = 394$ ft-lbs/rad.

Figure 6.- Comparison of theoretical and wind tunnel roll response of the model to an initial roll displacement.

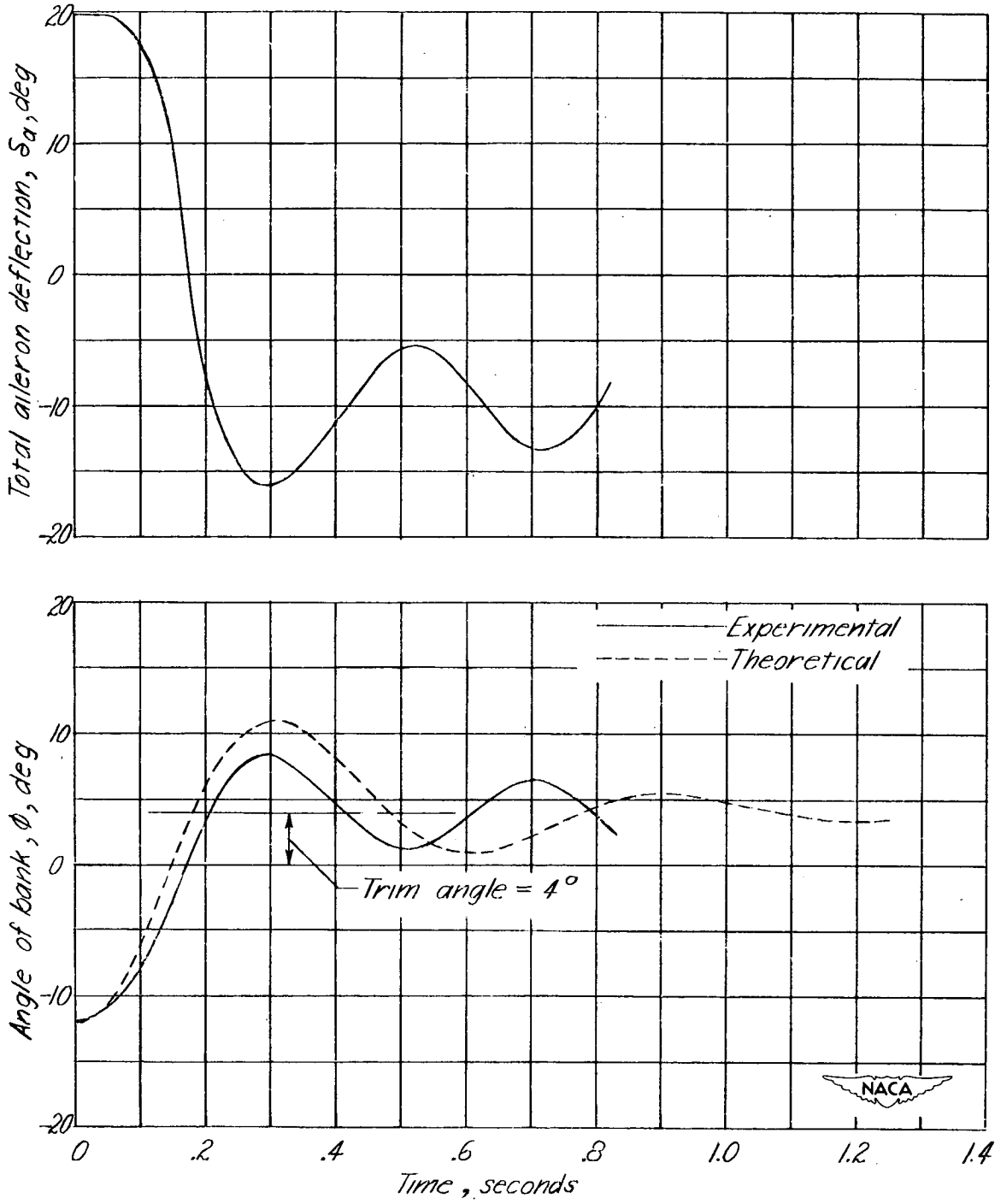

(b.) $K=2$, $M=0.6$; $L_{\dot{\phi}} = -37.67$ ft-lbs/rad/sec; $L_{\delta_a} = 407$ ft-lbs/rad.

Figure 6.- Continued.

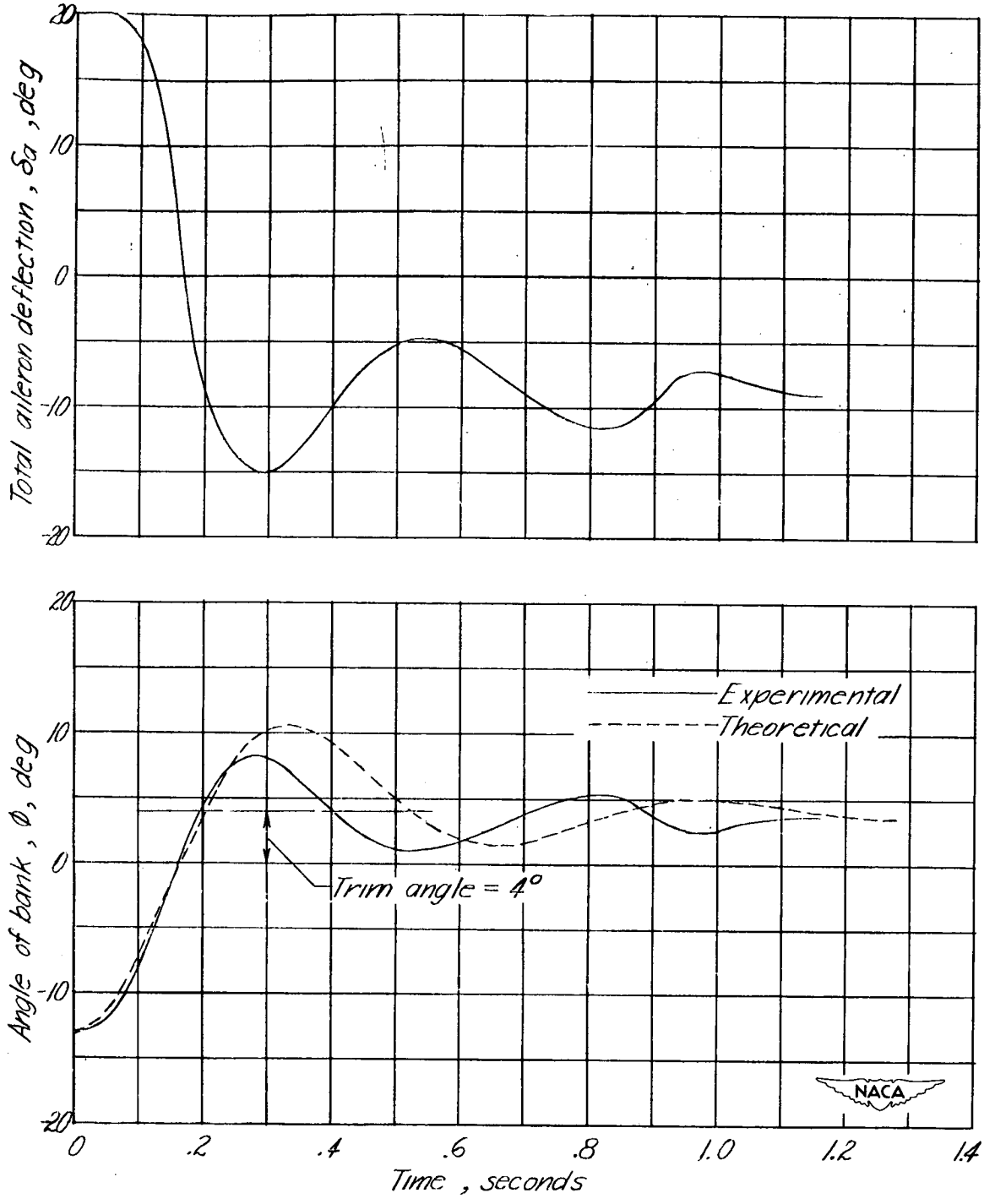

(c) $K=2$; $M=0.66$, $L_{\dot{\phi}} = -40.75$ ft-lbs/rad/sec; $L_{\delta a} = 358$ ft-lbs/rad.

Figure 6.- Continued.

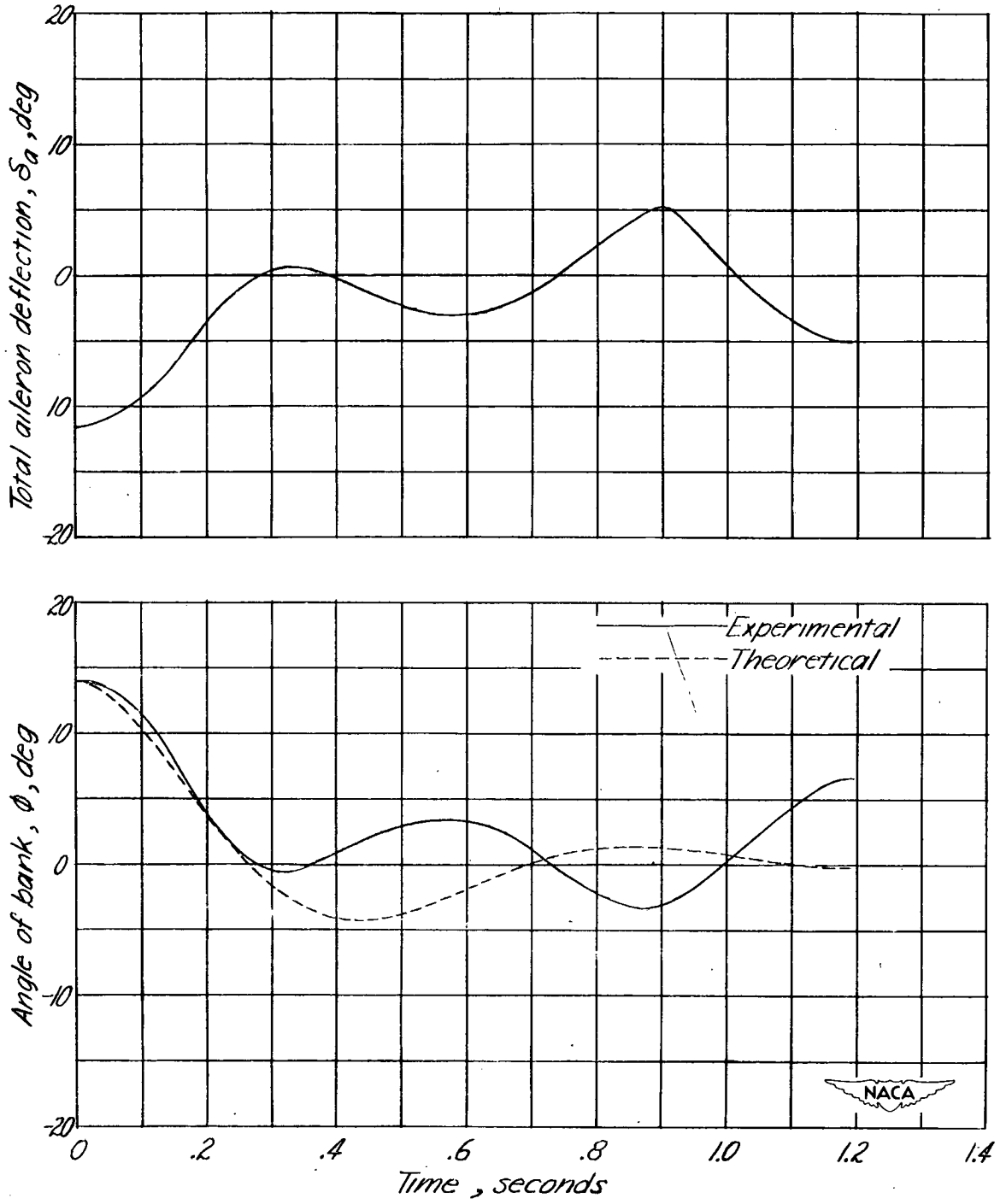

(d) $K=1$; $M=0.6$; $L_{\dot{\phi}} = -37.67$ ft-lbs/rad/sec; $L_{\delta_a} = 407$ ft-lbs/rad.

Figure 6.- Continued.

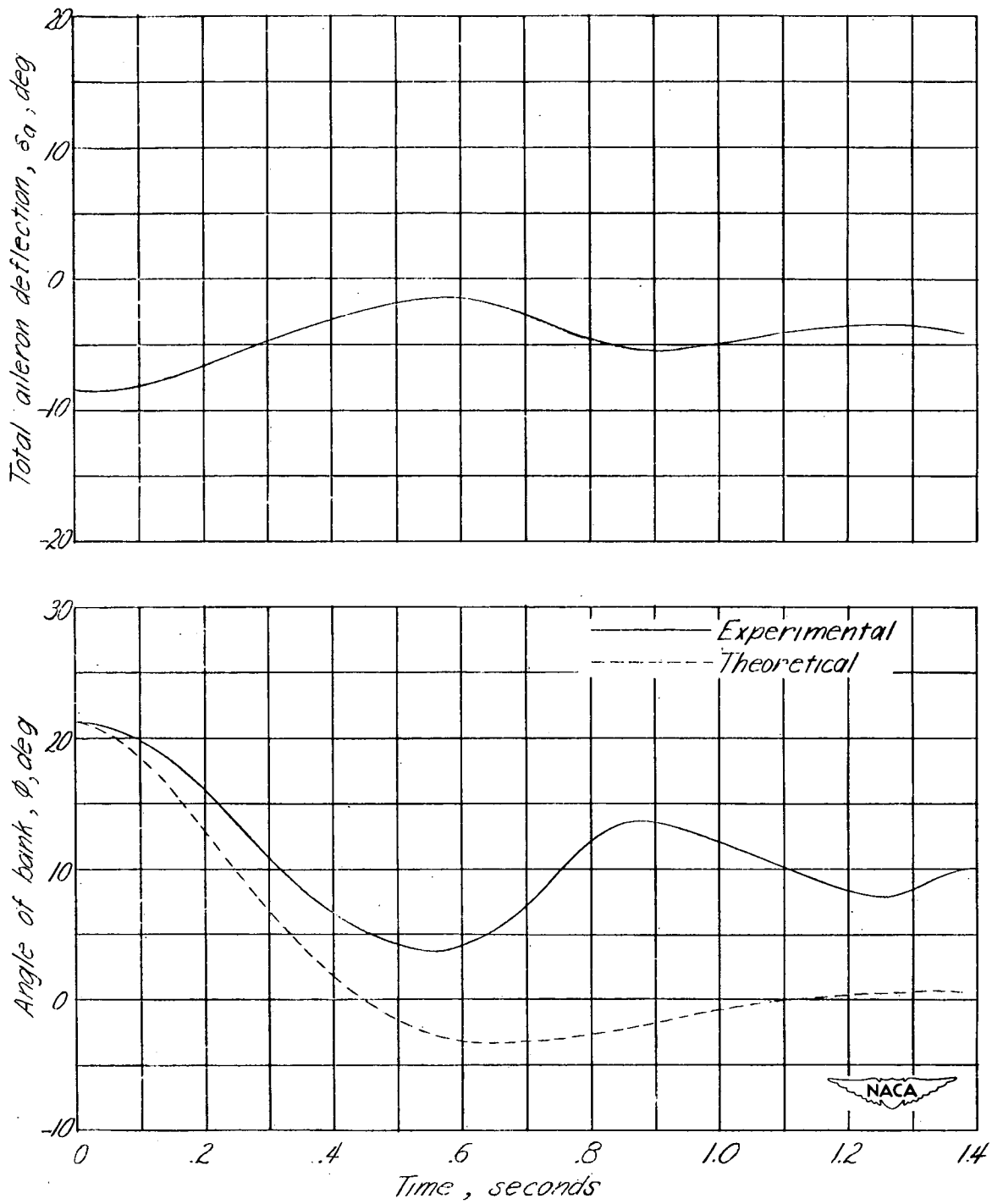

(e) $K=\frac{1}{2}$; $M=0.6$; $L_{\dot{\phi}} = -37.67$ ft-lbs/rad/sec; $L_{\delta_a} = 407$ ft-lbs/rad.

Figure 6.- Concluded.

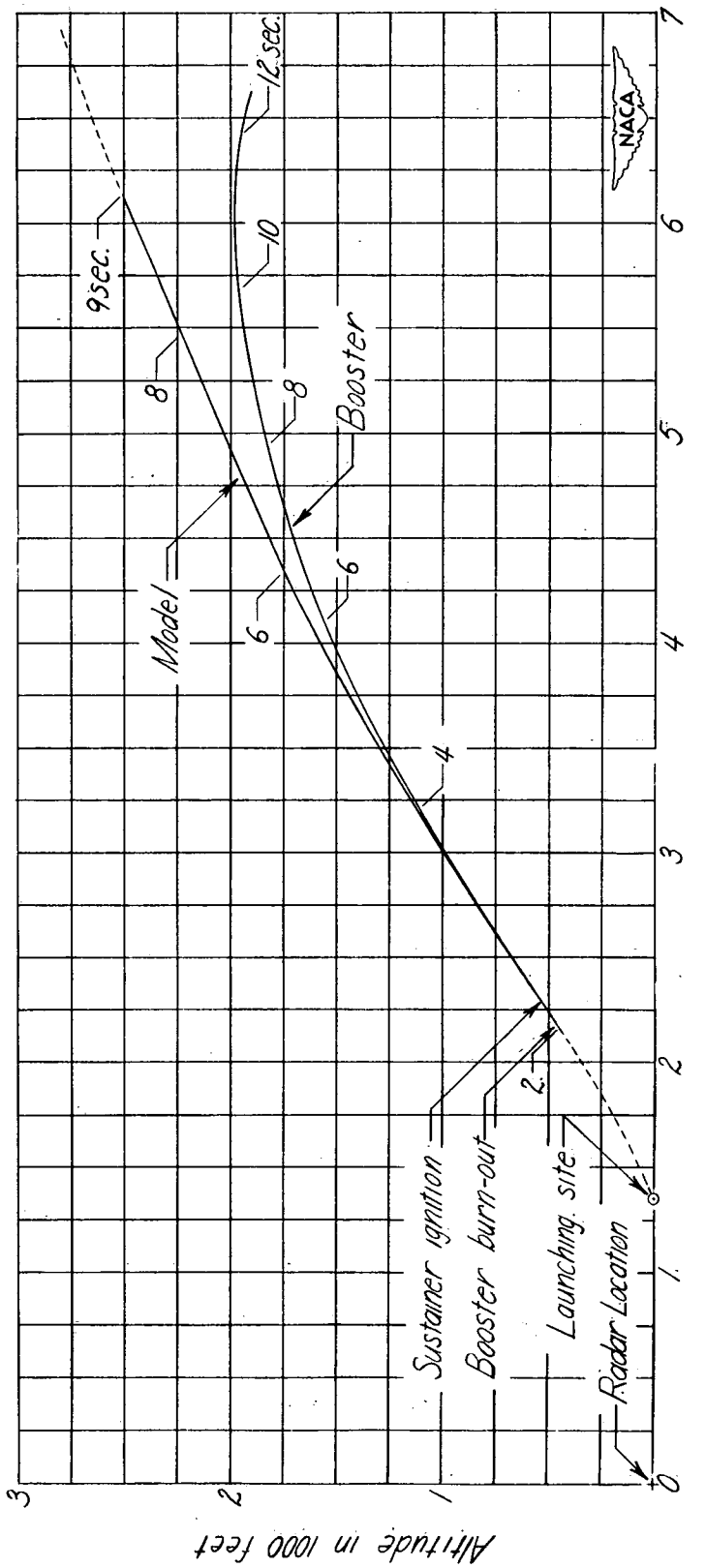

Figure 7. - Profile view of flight path of the model.

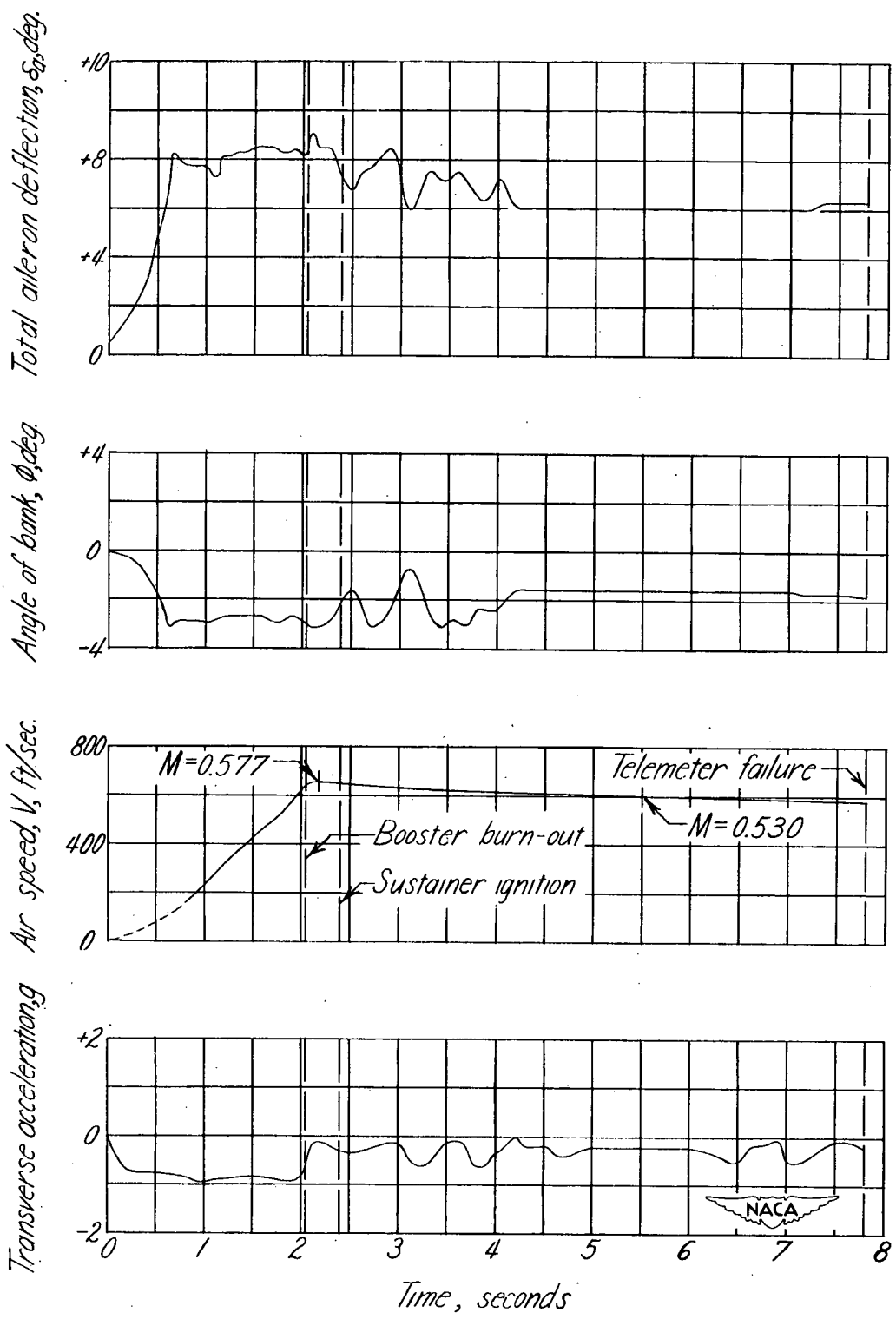

Figure 8.- Telemeter data of flight of the model.